Inorganic Chemistry

ARTICLE

pubs.acs.org/IC

# Ruthenium Hydride Complexes of the Hindered Phosphine Ligand Tris(3-diisopropylphosphinopropyl)phosphine

Mohan M. Bhadbhade,[‡] Leslie D. Field,[*,†] Ryan Gilbert-Wilson,[†] Ruth W. Guest,[§] and Paul Jensen[§]

[†]School of Chemistry and [‡]Mark Wainwright Analytical Centre, The University of New South Wales, NSW 2052, Australia

[§]School of Chemistry, University of Sydney, NSW 2006, Australia

Supporting Information

**ABSTRACT:** The synthesis and characterization of the novel hindered tripodal phosphine ligand $P(CH_2CH_2CH_2P^iPr_2)_3$ ($P^3P_3{}^{iPr}$) (**1**) are reported, along with the synthesis and characterization of ruthenium chloro and hydrido complexes of **1**. Complexes $[RuCl(P^3P_3{}^iPr)][BPh_4]$ (**2**[**BPh**$_4$]), $RuH_2(P^3P_3{}^iPr)$ (**3**), and $[Ru(H_2)(H)(P^3P_3{}^{iPr})][BPh_4]$ (**4**[**BPh**$_4$]) were characterized by crystallography. Complex **2** is fluxional in solution, and low-temperature NMR spectroscopy of the complex correlates well with two dynamic processes, an exchange between stereoisomers and a faster turnstile-type exchange within one of the stereoisomers.

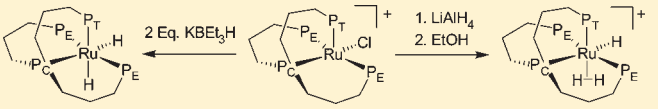


## INTRODUCTION

Polydentate phosphines have become important ligands for controlling the stereochemistry of coordination complexes and have also been used to solubilize metal catalysts.[1] $PP_3$ ligands, such as $P((CH_2)_nPR_2)_3$ ($n$ = 2, 3; R= Me, Ph), form metal complexes with a range of applications, especially for complexes of iron and ruthenium. Applications have ranged from the stabilization of complexes containing $\eta^2$-dihydrogen to the formation of stable dinitrogen complexes with iron and ruthenium in both the 0 and +2 oxidation states.[2] The $PP_3$-type ligand provides a strong coordination environment and is able to coordinate to the metal at up to four points through the four phosphine donors. Binding to form complexes with octahedral, trigonal bipyramidal, and also square-pyramidal geometry is possible with $PP_3$-type ligands. In an octahedral system, coordination of $PP_3$-type ligands leaves two free coordination sites for other ligands, and these are geometry constrained by the ligand to be in a cis arrangement. It is known that a cis arrangement of two ligands is a necessity for some parts of common catalytic mechanisms, such as migratory insertion.[3] Thus $PP_3$-type complexes often have higher catalytic activity, compared to complexes with mono or bidentate ligands, which can form inactive isomers where the two reactive ligands are in the unreactive trans arrangement.[4]

The encapsulating nature of $PP_3$ ligands and the presence of sterically bulky groups on the terminal phosphines of $PP_3$ ligands also has the propensity to restrict access to the metal center and enhance chemical reaction at any of the non-$PP_3$ ligands.

There is now an expanding range of sterically encumbered, polydentate ligands available,[5] and we report here the synthesis of the hindered tripodal tetradentate phosphine ligand $P(CH_2CH_2CH_2P^iPr_2)_3$ ($P^3P_3{}^{iPr}$). This ligand is a more hindered version of the $PP_3$-type ligand skeleton, $P(CH_2CH_2CH_2PR_2)_3$ which is known with either ethyl or methyl substituents on the terminal phosphine donors.[6]

This work reports a reasonable synthetic route to the hindered ligand as well as the formation and characterization of the iron and ruthenium chloro and hydrido complexes. Characterization of these complexes allows analysis of the geometry around the metal center as well as provides an initial assessment of the chemistry of these metal complexes.

## RESULTS AND DISCUSSION

Syntheses of other $PP_3$-type ligands with propylene bridges between the apical and terminal phosphines have usually involved the radical-initiated addition of a dialkylphoshine ($R_2P-H$) across the double bond of triallylphosphine. Syntheses of both $P(CH_2CH_2CH_2PMe_2)_3$ and $P(CH_2CH_2CH_2PEt_2)_3$ have been reported using this general approach.[6e] While $P(CH_2CH_2CH_2P^iPr_2)_3$ (**1**) can be synthesized by this approach, the long reaction time and the tendency to form $P^iPr_2CH_2CH_2CH_2P^iPr_2$ as a reaction side product make it a less than ideal synthesis.

$P^3P_3{}^iPr$ (**1**) can be synthesized more efficiently using an alternative approach via nucleophilic substitution of the halide in tris(3-bromopropyl)phosphine with a dialkylphosphide (Scheme 1). Tris(3-hydroxypropyl)phosphine was brominated using phosphorus tribromide to give the unstable tris(3-bromopropyl)phosphine. Tris(3-bromopropyl)phosphine tends to form a mixture of oligomeric and polymeric products on standing, probably by intramolecular or intermolecular nucleophilic attack of the central phosphine on a brominated $\gamma$-carbon, to form an insoluble solid mass within a few hours. Tris(3-bromopropyl)phosphine was used immediately in the next step of the sequence without further purification. $P(CH_2CH_2CH_2P^iPr_2)_3$, $P^3P_3{}^{iPr}$ (**1**) was prepared in moderate yield

**Received:** March 9, 2011
**Published:** June 01, 2011

  

(51% from tris(3-hydroxypropyl)phosphine) by the nucleophilic substitution of bromide in the reaction of lithium diisopropylphosphide, ($LiP^iPr_2$) with tris(3-bromopropyl)phosphine (Scheme 1). This method of synthesis is relatively direct and clean and avoids the difficulty of the alternative radical route which typically requires prolonged reaction times with volatile and reactive secondary phosphines and the known formation of unwanted byproduct.[6e]

In the $^{31}P\{^1H\}$ spectrum of $P(CH_2CH_2CH_2P^iPr_2)_3$, $P^3P_3{}^{iPr}$ (**1**), two resonances are observed at 1.9 and −34.7 ppm, and these are assigned to the terminal phosphines and the central phosphine respectively. Both resonances are singlets with no discernible coupling between the two phosphine environments, and this is consistent with data reported for other $P^3P_3$-type ligands incorporating propylene bridges between the apical and terminal phosphines.[6e]

Tripodal phosphorus ligands of the $P((CH_2)_nPR_2)_3$ ($n = 2, 3$) type are well established as good ligands at ruthenium centers,[7] and in this work, the $P^3P_3{}^{iPr}$ ligand **1** was successfully employed in the synthesis of the five-coordinate chloro complex of ruthenium $[RuCl(P^3P_3{}^{iPr})]^+$ (**2**).

**$[RuCl(P^3P_3{}^{iPr})]^+$.** Addition of sodium tetraphenylborate to a tetrahydrofuran (THF) solution of $P^3P_3{}^{iPr}$ (**1**) and $RuCl_2(PPh_3)_3$ afforded $[RuCl(P^3P_3{}^{iPr})][BPh_4]$ (**2**[**BPh$_4$**]) as a pink solid (Scheme 2). Crystals suitable for structural analysis were grown from a THF/pentane solution of **2**[**BPh$_4$**] (Figure 1A), and selected bond angles and lengths are given in Table 1.

The two structures within the asymmetric unit are sufficiently similar that the crystallographic data of only one of the configurations, namely Ru1, is detailed here. Each asymmetric unit within the crystal structure contains one THF molecule, giving half a THF solvate for each metal complex.

The geometry of $[RuCl(P^3P_3{}^{iPr})]^+$ (**2**) is a distorted square-based pyramid with atoms Cl1, P1, P2, and P4 making up the base and P3 at the apex ($\tau = 0.13$).[8] In this instance, the $P_E-Ru-P_E$ angle, P1−Ru1−P4, at 156.51(2)° is appreciably closer to that of a square-based pyramid (180°) than a trigonal bipyramid (120°). In addition, the $Ru-P_T$ bond length, Ru1−P3, at 2.2536(6) Å is significantly shorter than the $Ru-P_E$ bond lengths Ru1−P1 and Ru1−P4 (2.4629(6) and 2.3892(7) Å, respectively), and this is characteristic of square-based pyramid geometry. One of the isopropyl methyl groups fills and blocks the void under the base of the pyramid probably through an anagostic (pseudoagostic) interaction ($d$(Ru−H) = 2.637 Å (Ru1) and 2.369 Å (Ru2); Ru−C−H = 127.75°(Ru1) and 131.18°(Ru2)).[9]

There are three structures of ruthenium with the analogous tripodal tetradentate ligand ($P(CH_2CH_2CH_2PMe_2)_3$),[10] however, these are all six-coordinate complexes with approximate octahedral geometry around the metal center.

The only comparative structure of a five-coordinate complex of ruthenium with a tripodal tetradentate phosphine ligand is that of $[RuCl(P(CH_2CH_2P^iPr_2)_3)][BPh_4]$,[2a] which can be approximated to a distorted square-based pyramid in the same way as **2** (included in Figure 1B for comparison). In a similar fashion to **2**, $[RuCl(P(CH_2CH_2P^iPr_2)_3)][BPh_4]$ also has one of the isopropyl

**Scheme 1**

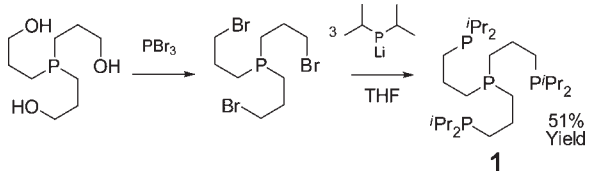


**Scheme 2**

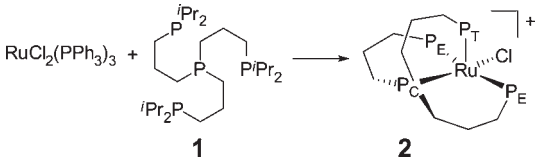


**Table 1. Selected Bond Lengths (Å) and Angles (°) for 2[RuCl(P$^3$P$_3{}^{iPr}$)][BPh$_4$]·THF (2[BPh$_4$])**

| | | | |
|---|---|---|---|
| Ru1−Cl1 | 2.4351(7) | Ru1−P2 | 2.2618(7) |
| Ru1−P1 | 2.4629(6) | Ru1−P3 | 2.2536(6) |
| Ru1−P4 | 2.3892(7) | | |
| Cl1−Ru1−P2 | 165.53(2) | Cl1−Ru1−P1 | 89.28(2) |
| Cl1−Ru1−P3 | 103.06(2) | Cl1−Ru1−P4 | 83.51(2) |
| P2−Ru1−P1 | 89.20(2) | P2−Ru1−P3 | 91.38(2) |
| P2−Ru1−P4 | 92.25(3) | P1−Ru1−P3 | 99.40(2) |
| P1−Ru1−P4 | 156.51(2) | P3−Ru1−P4 | 104.00(2) |

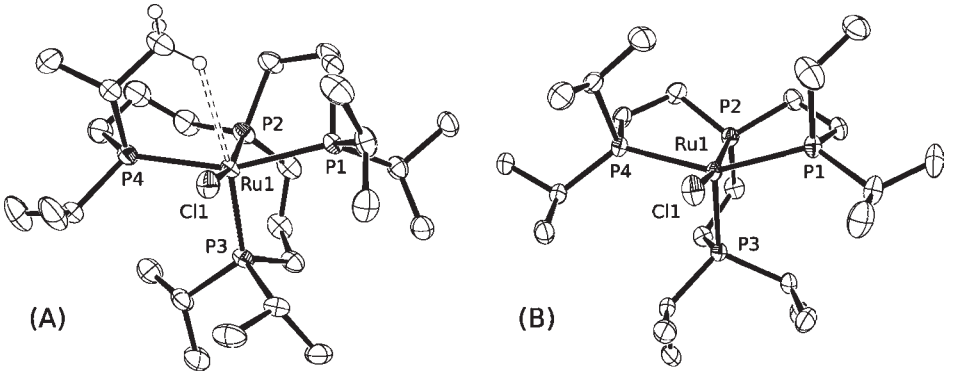


**Figure 1.** ORTEP plot (50% thermal ellipsoids) of: (A) 2[RuCl(P$^3$P$_3{}^{iPr}$)][BPh$_4$]·THF (2[BPh$_4$]) (see Supporting Information for more data) and for comparison (B) $[RuCl(P(CH_2CH_2P^iPr_2)_3)][BPh_4]$.[2a] Only one of the two complex cations in each asymmetric unit in shown. Selected hydrogen atoms, tetraphenylborate anions, and THF solvate have been omitted for clarity.


dx.doi.org/10.1021/ic200492w |Inorg. Chem. 2011, 50, 6220–6228

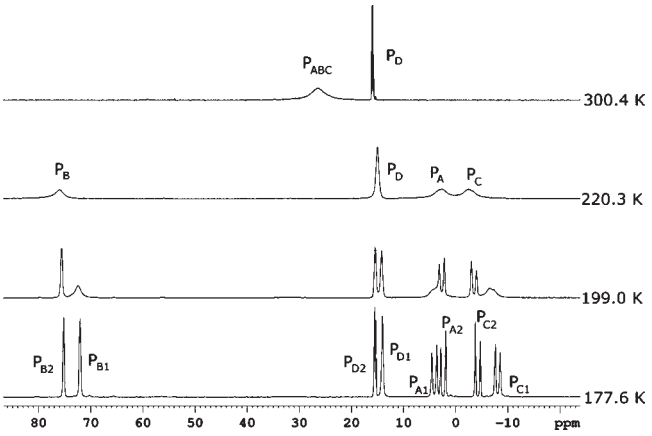


**Figure 2.** Variable-temperature $^{31}P\{^{1}H\}$ NMR spectra for $[RuCl(P^{3}P_{3}^{iPr})][BPh_4]$ (**2**[**BPh**$_4$]) (242.95 MHz, methylene chloride-$d_2$).

**Scheme 3**

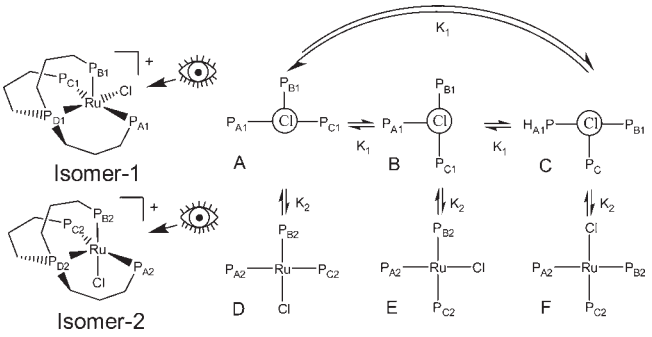


methyl groups filling and blocking the sixth coordination site under the base of the pyramid.

The metal-to-donor atom bond lengths of **2** are equivalent to, or longer than, the analogous lengths in $[RuCl(P(CH_2CH_2P^iPr_2)_3)]^+$. The P−Ru−P bond angles are all greater in **2**, and the Cl−Ru−P bond angles are all more acute than in $[RuCl(P(CH_2CH_2P^iPr_2)_3)]^+$. Thus in $[RuCl(P((CH_2)_n P^iPr_2)_3)]^+$ complexes with $n = 2, 3$, the complex with 3-carbon straps is a less strained complex and shows relaxation of the ligand bite angles and a lengthening of the metal-to-donor atom bond lengths.

In the $^{31}P\{^{1}H\}$ NMR spectrum of **2**[**BPh**$_4$] at room temperature, the signal for the three terminal phosphines appears as a very broad resonance at 25.7 ppm, while the signal for the central phosphine appears as a sharp quartet at 14.2 ppm with a splitting of 36.4 Hz. A modest increase (25 K) in the temperature of the NMR experiment resulted in an appreciable sharpening of the resonances of the terminal phosphines. These spectra are analogous to those of $[RuCl(P(CH_2CH_2P^iPr_2)_3)][BPh_4]$,[2a] and the broadness can be rationalized by the facile exchange of the terminal phosphine environments.

It is interesting to note that the central phosphine resonance in **2**[**BPh**$_4$] appears to high field with respect to the terminal phosphine signals. In the analogous compound with two-carbon straps $[RuCl(P(CH_2CH_2P^iPr_2)_3)][BPh_4]$, the $^{31}P\{^{1}H\}$ NMR spectrum shows the central phosphine as a quartet at 142.9 ppm (splitting 15.2 Hz) to low field of the three terminal

**Scheme 4**

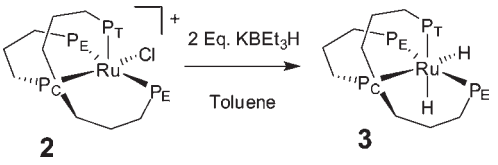


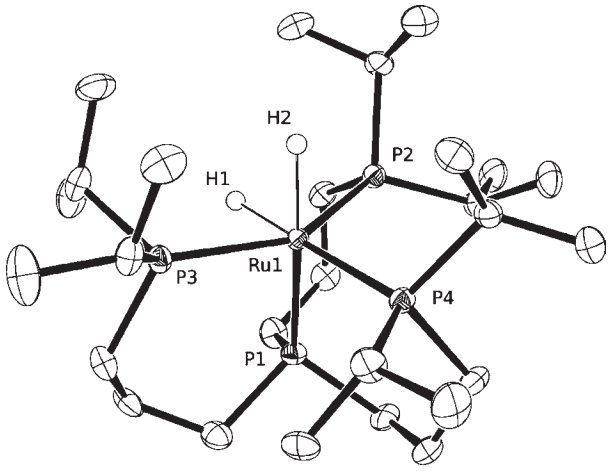


**Figure 3.** ORTEP plot (50% thermal ellipsoids) of one of the two $[RuH_2(P^3P_3^{iPr})]$ (**3**) units within the asymmetric unit. Selected hydrogen atoms have been removed for clarity.

phosphines, displayed as an exchange-broadened singlet at 72.1 ppm. The reversal in relative chemical shifts from **2** to those of $[RuCl(P(CH_2CH_2P^iPr_2)_3)][BPh_4]$ is rationalized by the five-membered ring effect in phosphorus metallocycles. The 5-membered ring effect is reasonably well documented and describes how phosphorus nuclei involved in 5 member metallocycles are significantly shifted to downfield compared to their 4, 6, and 7 member metallocycle anaologues.[11] This effect is magnified for the central phosphorus $P_C$ in $[RuCl(P(CH_2CH_2P^iPr_2)_3)]$ since the central P is effectively part of three five-membered metallocycles, and this rationalizes why the two complexes, while chemically and structurally similar, have $^{31}P$ chemical shifts for the central P atom which differ by almost 130 ppm.

As the temperature of the $^{31}P\{^{1}H\}$ NMR spectrum of **2**[**BPh**$_4$] is decreased, the spectra broaden and then sharpen (Figure 2). At 243 MHz, as the temperature decreases to 220 K, the single broad resonance for the terminal phosphines separates into three distinct resonances representing the terminal phosphines individually, giving four distinct resonances representing the four different phosphine environments. At still lower temperatures, each of the resonances eventually splits into two resonances of comparable intensity (1:0.8) to give a total of 8 resonances, which we attribute to two isomers of **2**[**BPh**$_4$]. The Cl resides either trans to the apical phosphorus or trans to a terminal phosphorus (Isomer-1 and Isomer-2) (Scheme 3).

In this system there are two exchange processes operating. One which exchanges the terminal phosphorus environments, and one which interchanges Isomer-1 and Isomer-2. At 199 K, the three resonances of the terminal phosphines of Isomer-2


dx.doi.org/10.1021/ic200492w |*Inorg. Chem.* 2011, 50, 6220–6228

($P_{A2}$, $P_{B2}$, $P_{C2}$) resolve with $^2J_{P-P}$ coupling observed, while in Isomer-1 the terminal phosphine resonances remain broad with no defined coupling. All of the resonances eventually sharpen at 178 K to display similar coupling patterns.

The fact that the resonances of one isomer sharpen while the resonances of the other remain broad suggests that the exchange of the terminal phosphines is faster in one isomer (Isomer-1) than in the other. The pattern and sequence of coalescences in the variable temperature NMR spectra can be rationalized by a model where exchange between the terminal phosphines in Isomer-1 ($k_1$) is fast compared to the interchange between the isomers ($k_2$, Scheme 3). We suggest that Isomer-1 is that in which Cl is trans to the central phosphines since the exchange of the terminal phosphines then involves simply a turnstile-type process, with exchange of the terminal phosphines between adjacent coordination sites.

**Table 2. Selected Bond Lengths (Å) and Angles (°) for [$RuH_2(P^3P_3{}^{iPr}$)] (3)**

| | | | |
|---|---|---|---|
| Ru1 -H1 | 1.62(5) | Ru1 −H2 | 1.69(5) |
| Ru1 −P1 | 2.2785(13) | Ru1 −P2 | 2.3162(12) |
| Ru1 −P4 | 2.3502(12) | Ru1 −P3 | 2.3032(12) |
| H1−Ru1−P2 | 71.7(17) | H1−Ru1−P1 | 85.1(19) |
| H1−Ru1−P3 | 75.4(17) | H1−Ru1−P4 | 176.7(18) |
| H2−Ru1−P2 | 88.4(15) | H2−Ru1−P1 | 175.7(16) |
| H2−Ru1−P3 | 85.0(15) | H2−Ru1−P4 | 90.7(16) |
| P2−Ru1−P1 | 89.45(4) | P2−Ru1−P3 | 146.44(4) |
| P2−Ru1−P4 | 105.33(4) | P1−Ru1−P3 | 94.75(4) |
| P1−Ru1−P4 | 93.42(4) | P3−Ru1−P4 | 107.62(4) |
| H1−Ru1−H2 | 91(2) | | |

Simulation[12] of the exchange-broadened $^{31}P\{^1H\}$ NMR spectrum of [$RuCl(P^3P_3{}^{iPr}$)][$BPh_4$] (**2**[**$BPh_4$**]) was consistent with an exchange process where $k_1 \approx 3.5k_2$, and at 199 K, $k_1 \approx 385$ and $k_2 \approx 110\ s^{-1}$ and at 210 K with $k_1 \approx 2135$ and $k_2 \approx 610\ s^{-1}$.

**$RuH_2(P^3P_3{}^{iPr})$.** Reaction of the ruthenium chloro complex [$RuCl(P^3P_3{}^{iPr}$)][$BPh_4$] (**2**[**$BPh_4$**]) with two equivalents of $KBEt_3H$ afforded the dihydride complex $RuH_2(P^3P_3{}^{iPr})$ (**3**) as a white crystalline solid (Scheme 4). Crystals suitable for structural analysis were grown by slow evaporation of a toluene solution of **3** under nitrogen (Figure 3) and selected bond angles and lengths are given in Table 2.

The geometry of $RuH_2(P^3P_3{}^{iPr})$ (**3**) is a distorted octahedron with the two hydrides in mutually cis coordination sites. There are eight previously reported structures of ruthenium(II) tetraphosphine dihydrides of which four have defined and refined hydrides.[10c,13] The Ru−H bond lengths of 1.62(5) and 1.69(5) Å sit comfortably within the ranges provided by the other 4 structures, with Ru−H bond lengths of 1.51 to 1.77 Å. Similarly the H−Ru−H bond angle of 91(2)° sits within the range of previously reported structures with bond angles between 77 to 93°.

The structure of **3** is analogous to that of [$RuH_2$-($P(CH_2CH_2CH_2PMe_2)_3$)],[10c] which contains the related tetradentate phosphine ligand with methyl substituents on the terminal phosphines instead of isopropyl substituents. The average of the Ru−P bond lengths, 2.312 Å is slightly longer than for [$RuH_2(P(CH_2CH_2CH_2PMe_2)_3)$] for which the average Ru−P bond length is 2.286 Å. This is probably due to the steric bulk of the isopropyl substituents when compared to the methyl substituents, resulting in elongation of the core Ru−P bonds.

In the $^{31}P\{^1H\}$ NMR spectrum of $RuH_2(P^3P_3{}^{iPr})$ (**3**), the signal for the two terminal phosphines $P_E$ appears as a doublet of

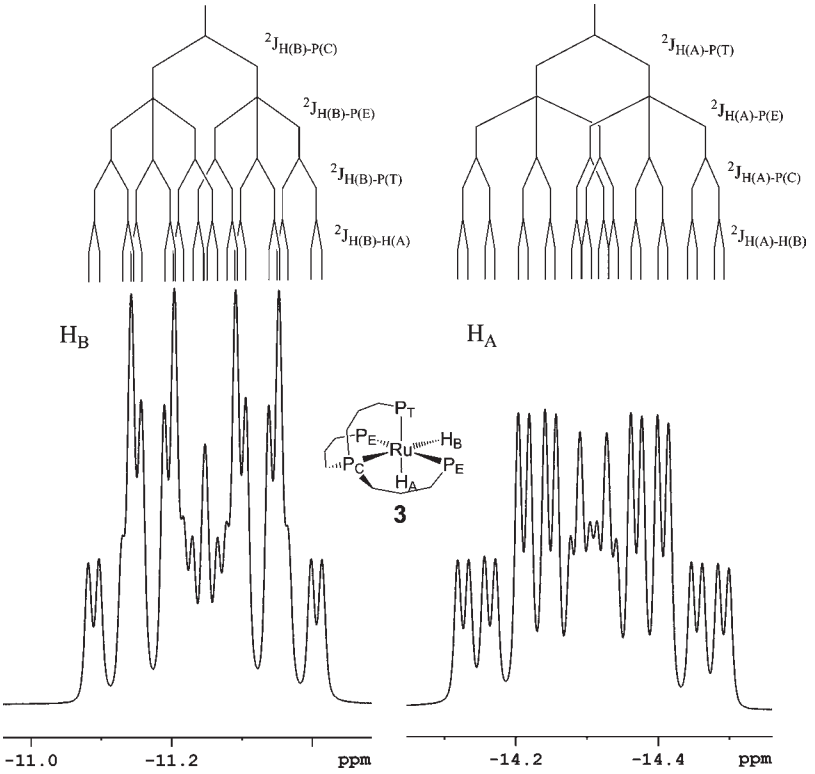


**Figure 4.** Selected high-field region of $^1H$ NMR (600 MHz, benzene-$d_6$) $RuH_2(P^3P_3{}^{iPr})$ (**3**) with coupling tree.


dx.doi.org/10.1021/ic200492w |*Inorg. Chem.* 2011, 50, 6220–6228

Scheme 5

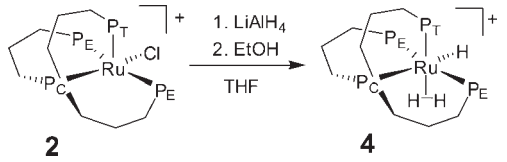


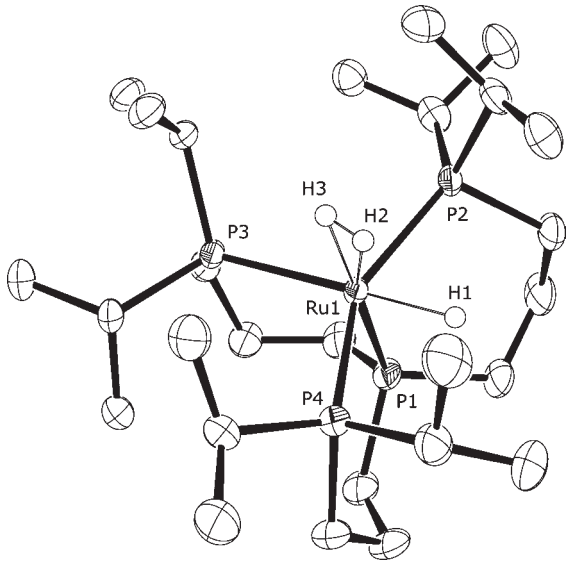


**Figure 5.** ORTEP plot (50% thermal ellipsoids) of the complex cation of $[Ru(H_2)(H)(P^3P_3^{iPr})][BPh_4]\cdot EtOH$ (**4**[**BPh**$_4$]) (see Supporting Information for more data) within the asymmetric unit. Selected hydrogen atoms have been removed for clarity.

doublets at 49.2 ppm, the signal for the terminal phosphine $P_T$ is a doublet of triplets at 28.5 ppm, and the central phosphine $P_C$ signal appears as a doublet of triplets at 0.4 ppm.

The $^1$H NMR resonances for the two hydrido ligands of **3** both appear as doublets of triplets of doublets of doublets at −9.43 and −12.50 ppm due to coupling to the 4 phosphorus nuclei in 3 different environments and to each other (Figure 4). The coupling constants $^2J_{H-P}$ are 59.6 Hz, 24.2 and 18.8 Hz for the resonance at −9.43 ppm and 63.2 Hz, 34.0 and 15.0 Hz for the resonance at −12.50 ppm, with the $^2J_{H-H}$ coupling constant between the two hydrides of 6.2 Hz.

**[Ru(H$_2$)(H)(P$^3$P$_3^{iPr}$)][BPh$_4$].** A solution of $LiAlH_4$ (∼1.5 M) in THF was added dropwise to a THF solution of **2**[**BPh**$_4$] to the point where the color change from pink to colorless was complete. Ethanol was added, and the resulting orange suspension worked up to afford $[Ru(H_2)(H)(P^3P_3^{iPr})][BPh_4]$ **4**[**BPh**$_4$] as an orange crystalline solid (Scheme 5). Crystals suitable for structural analysis were grown from a THF/pentane solution of **4**[**BPh**$_4$] (Figure 5), and selected bond angles and bond lengths are given in Table 3.

The geometry of $[Ru(H_2)(H)(P^3P_3^{iPr})]^+$ (**4**) is a distorted octahedral with the hydride and dihydrogen ligands in mutually cis coordination sites. There are two other structures of dihydrogen hydrido ruthenium complexes where the hydrido and dihydrogen ligands are in the cis arrangement with four other phosphine donors, $[Ru(H_2)(H)(PPh_2Me)_4]$[14] and $[Ru(H_2)(H)(P(CH_2CH_2PPh_2)_3)]^+$.[15] In both of these complexes, the

**Table 3. Selected Bond Lengths (Å) and Angles (°) for [Ru(H$_2$)(H)(P$^3$P$_3^{iPr}$)][BPh$_4$].EtOH 4[BPh$_4$]**

| | | | |
|---|---|---|---|
| H2 −H3 | 0.66(6) | Ru1 −H1 | 1.59(3) |
| Ru1 −H2 | 1.62(6) | Ru1 −H3 | 1.75(4) |
| Ru1 −P1 | 2.2890(9) | Ru1 −P2 | 2.3756(9) |
| Ru1 −P3 | 2.4270(8) | Ru1 −P4 | 2.3591(9) |
| H1−Ru1−H2 | 75(2) | H1−Ru1−H3 | 97.4(18) |
| H2−Ru1−H3 | 23(2) | H1−Ru1−P1 | 86.3(12) |
| H1−Ru1−P2 | 75.1(12) | H1−Ru1−P3 | 178.7(12) |
| H1−Ru1−P4 | 74.1(12) | H2−Ru1−P1 | 161(2) |
| H2−Ru1−P2 | 89(2) | H2−Ru1−P3 | 106(2) |
| H2−Ru1−P4 | 79(2) | H3−Ru1−P1 | 175.4(14) |
| H3−Ru1−P2 | 89.2(13) | H3−Ru1−P3 | 89.2(13) |
| H3−Ru1−P4 | 90.1(13) | P1−Ru1−P2 | 89.15(3) |
| P1−Ru1−P3 | 92.36(3) | P1−Ru1−P4 | 93.56(3) |
| P2−Ru1−P3 | 104.61(3) | P2−Ru1−P4 | 148.79(3) |
| P3−Ru1−P4 | 106.33(3) | | |

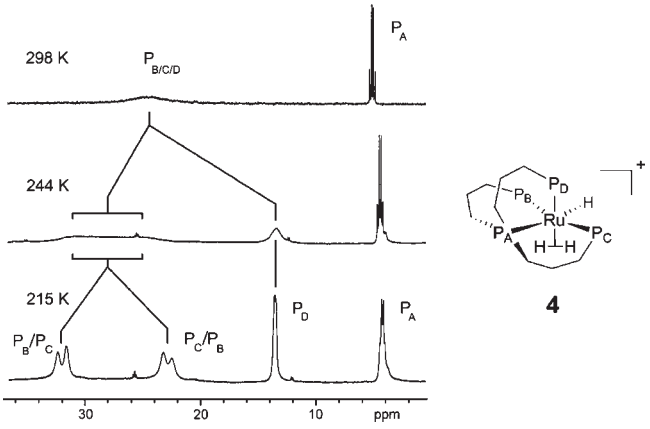


**Figure 6.** $^{31}P\{^1H\}$ NMR spectrum (242.9 MHz, THF-$d_8$) of $[Ru(H_2)(H)(P^3P_3^{iPr})][BPh_4]$ (**4**[**BPh**$_4$]) at 298, 244, and 215 K.

dihydrogen ligand was not refined. There have, however, been examples of ruthenium cis hydride dihydrogen complexes with all ligands refined, including the dihydrogen ligand, and these include $[Ru(H)(H_2)(X)(P^iPr_3)_2]$ (X = benzoquinoline, **5**)[16] and $[RuH(H_2)(o\text{-}C_6H_5py)(P^iPr_3)_2][BArf]$ **6**[**BArF**].[17] The Ru1−H1 bond length for **4** (1.59(3) Å) is comparable to that of **5** (1.54(4) Å) and **6**[**BArF**] (1.528(20) Å). Likewise the dihydrogen bond distances Ru1−H2 and Ru−H3 for **4** of 1.62(6) and 1.75(4) Å, respectively, are similar but slightly elongated compared to those for **5** (1.57(5) and 1.68(4) Å) and **6**[**BArF**] (1.564(20) and 1.547(21) Å). This elongation is probably caused by the differences in the donor atom in the coordination site trans to dihydrogen, with **5** being carbon and **6**[**BArF**] being nitrogen as opposed to phosphorus in **4**.

$[Ru(H_2)(H)(P^3P_3^{iPr})][BPh_4]$ (**4**[**BPh**$_4$]) is clearly fluxional in solution. At low temperature (215 K) there are 4 resonances for the coordinated phosphines (at 30.3, 21.3, 13.7, and 4.3 ppm, Figure 6). The appearance of four resonances is consistent with the solid-state structure where the two mutually trans phosphines are not equivalent due to puckering of the six-membered metallocyclic rings. At low temperature, the two mutually trans phosphines ($P_B$ and $P_C$) exhibit a large resolved


dx.doi.org/10.1021/ic200492w |Inorg. Chem. 2011, 50, 6220–6228

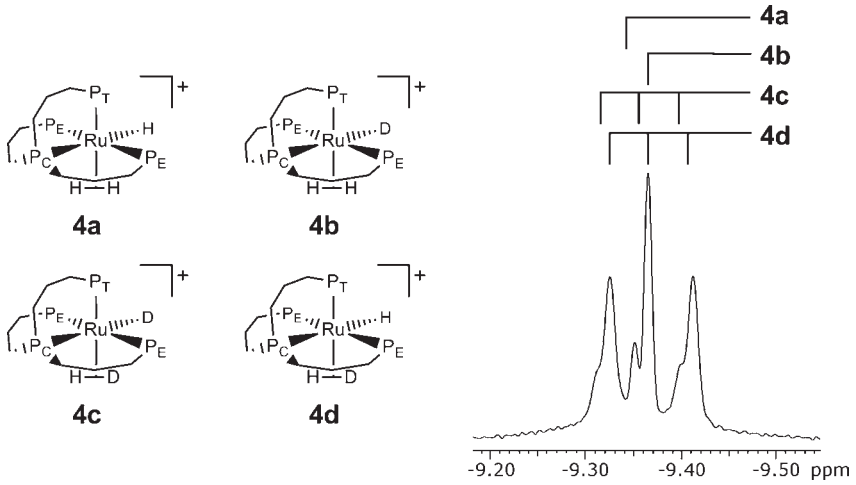


**Figure 7.** Selected high-field $^{1}H\{^{31}P\}$ NMR spectrum (700 MHz, THF-$d_8$) of partially deuterated $[Ru(H_2)(H)(P^3P_3^{iPr})][BPh_4]$ (**4**[**BPh$_4$**]) at 200 K with resolution enhancement.

**Table 4. Crystal Data Refinement Details for 2[BPh$_4$], 3, and 4[BPh$_4$]**

| | 2[BPh$_4$] | 3 | 4[BPh$_4$] |
|---|---|---|---|
| chemical formula | $C_{104}H_{168}OB_2Cl_2P_8Ru_2$ | $C_{27}H_{62}P_4Ru$ | $C_{52}H_{86}BOP_4Ru$ |
| formula mass | 2000.82 | 611.72 | 956.94 |
| crystal system | triclinic | monoclinic | monoclinic |
| $a$/Å | 12.280(2) | 17.099(2) | 16.4283(7) |
| $b$/Å | 19.093(4) | 17.3858(17) | 17.7729(6) |
| $c$/Å | 23.928(4) | 21.692(3) | 18.1170(6) |
| α/° | 111.889(3) | 90.00 | 90.00 |
| $\beta$/° | 98.687(3) | 100.723(4) | 105.8920(10) |
| $\gamma$/° | 90.272(3) | 90.00 | 90.00 |
| $V$ (Å$^3$) | 5134.6(16) | 6335.9(13) | 5087.6(3) |
| temperature/K | 150(2) | 150(2) | 150(2) |
| space group | $P\bar{1}$ | $P2(1)/c$ | $P2(1)/n$ |
| $Z$ | 2 | 8 | 4 |
| $\mu$(Mo Kα) (mm$^{-1}$) | 0.517 | 0.711 | 0.468 |
| $N$ | 49295 | 43788 | 60050 |
| $N_{ind}$ | 23041 | 11053 | 11063 |
| $R_{int}$ | 0.0245 | 0.0999 | 0.0561 |
| Final $R_1$ values ($I > 2\sigma(I)$) | 0.0322 | 0.0426 | 0.0468 |
| Final $wR(F^2)$ values ($I > 2\sigma(I)$) | 0.0754 | 0.1098 | 0.0975 |
| Final $R_1$ values (all data) | 0.0496 | 0.0770 | 0.0670 |
| Final $wR(F^2)$ values (all data) | 0.0851 | 0.1417 | 0.1054 |
| Goodness of fit on $F^2$ | 1.034 | 0.790 | 1.095 |

coupling (about 180 Hz). As the temperature is raised to 244 K, the resonances for $P_B$ and $P_C$ broaden and coalesce, and this is probably due to ring-flipping of the ligand backbone. At higher temperatures (above 298 K), there is mutual exchange of all three of the terminal phosphines (a turnstile-type exchange), and the signals for the terminal phosphines are averaged to a single broad resonance. Modeling of the exchanges at 244 K indicates that the exchange of magnetism between the mutually trans phosphines (ring flip) occurs at a rate of about 3000 s$^{-1}$ and that the turnstile exchange of the terminal phosphines occurs at a significantly slower rate (about 300 s$^{-1}$).

At 298 K, the $^1$H NMR resonances of the hydrido and dihydrogen ligands of **4**[**BPh$_4$**] appear as a single broad resonance at −8.57 ppm, indicating fast exchange between the hydrido and dihydrogen ligands. At 195 K the signal resolves to a broad 2-proton resonance at −7.44 ppm, assigned to the dihydrogen ligand and a phosphorus-coupled doublet of triplets at −10.3 ppm ($^2J_{H-P}$ of 57 and 32 Hz) for the hydrido resonance. Further evidence for this assignment comes from the $T_1$ values for these two high field resonances at 180 K with the dihydrogen resonance having a $T_1$ of 68 ± 3 ms and the hydrido resonance a $T_1$ of 594 ± 12 ms. It is characteristic of dihydrogen hydrido metal complexes that the dihydrogen


dx.doi.org/10.1021/ic200492w |*Inorg. Chem.* 2011, 50, 6220–6228

ligand has a significantly faster relaxation time than the hydrido ligand.[6a]

Under an atmosphere of deuterium gas, the dihydrogen ligand exchanges for $D_2$, partially incorporating deuterium into the metal-bound hydrogens. In the $^1$H NMR spectrum at 200 K, the dihydrogen (or hydrogen deuteride) resonance at about −10 ppm appears as a superimposition of signals (Figure 7) due to the different isotopomers. The two 3-line resonances corresponding to the species with coordinated H−D can be resolved and the $J_{HD}$ coupling of 31 Hz extracted. $J_{HD}$ greater than 15 Hz is considered to be characteristic of dihydrogen complexes,[18] clearly confirming the presence of $\eta^2$-coordinated H−D in this species. Using the most recent interrelationship between H−H bond distance ($d_{HH}$) and H−D coupling ($J_{HD}$) of $d_{HH}$ = 1.47−0.0175 $J_{HD}$ Å determined by Gusev,[19] $d_{HH}$ is determined to be 0.927 Å. This is longer than the value determined from the crystal structure of $[Ru(H_2)(H)(P^3P_3{}^{iPr})][BPh_4]$ (**4**[**BPh$_4$**]) of 0.66(6) Å but expected, as crystallographic techniques are notorious for giving foreshortened $d_{HH}$ because of rapid $H_2$ rotation/vibration.[18]

$[Ru(H_2)(H)(P^3P_3{}^{iPr})][BPh_4]$ (**4**[**BPh$_4$**]) is remarkably stable and survives unchanged under a nitrogen atmosphere indefinitely without substitution of the $H_2$, even after several freeze−pump−thaw cycles. The lack of ready $N_2$ substitution probably reflects the fact that steric crowding from the bulky $P^3P_3{}^{iPr}$ ligand makes binding the smaller $H_2$ more preferable than the bulkier $N_2$.

Treatment of $[Ru(H_2)(H)(P^3P_3{}^{iPr})][BPh_4]$ (**4**[**BPh$_4$**]) with potassium *tert*-butoxide in $d_8$-THF results in clean deprotonation and formation of $RuH_2(P^3P_3{}^{iPr})$ (**3**). Conversely, treatment of **3** with triflic acid in $d_8$-THF in the presence of $BPh_4^-$ results in formation of **4**[**BPh$_4$**], and this acid/base behavior is consistent with that observed for other hydrido and dihydrido complexes of ruthenium and iron.[20]

## CONCLUSIONS

The new sterically hindered, tripodal tetradentate ligand $P^3P_3{}^{iPr}$ (**1**) was synthesized and used in the synthesis of a series of stable ruthenium compounds. The 5-coordinate chloro complex $[RuCl(P^3P_3{}^{iPr})]^+$ (**2**) was characterized crystallographically and by multinuclear NMR spectroscopy, with low-temperature $^{31}P\{^1H\}$ NMR spectroscopy being used to explore the exchange mechanisms between its various isomers. Complex **2** was reacted with potassium triethylborohydride to produce $RuH_2(P^3P_3{}^{iPr})$ (**3**). Complex **2** was also reacted with lithium aluminum hydride, followed by reaction with ethanol to produce the stable hydrido dihydrogen species $[Ru(H_2)(H)(P^3P_3{}^{iPr})]^+$ (**4**). Complexes **3** and **4** were characterized both crystallographically and by multinuclear NMR spectroscopy.

The bulky $P^3P_3{}^{iPr}$ ligand is among the most sterically encumbered $PP_3$-type ligands so far synthesized. While the $P^3P_3{}^{iPr}$ ligand, outlined in this paper, forms stable tetradentate 5- and 6-coordinate complexes with ruthenium, the complexes are hindered, and they are fluxional and hemilabile in solution. This behavior is typical of many complexes where the metal−P bonds are weakened because the bulky ligand substituents restrict the phosphorus donors from gaining optimal access to the metal center.

The synthetic approach to the $P^3P_3{}^{iPr}$ ligand is generic, and it is possible to introduce a range of substituents on the terminal phosphorus using this method. Other bulkier and tailored substituents may permit the chemistry of $PP_3$ metal complexes to be tuned to access catalytic reactivity not possible with stronger ligand sets.

## EXPERIMENTAL SECTION

**General Information.** All manipulations were carried out using standard Schlenk and glovebox techniques under a dry atmosphere of nitrogen. Solvents were dried and distilled under nitrogen or argon using standard procedures[21] and stored in glass ampules fitted with Youngs Teflon taps. Benzene was dried over sodium wire before distillation from sodium/benzophenone, while ethanol was distilled from diethoxymagnesium. THF (inhibitor free) and pentane were dried and deoxygenated using a Pure Solv 400-4-MD (Innovative Technology) solvent purification system. Deuterated solvents THF-$d_8$, toluene-$d_8$, and benzene-$d_6$ were dried over and distilled from sodium/benzophenone and were vacuum distilled immediately prior to use. Dichlorotris(triphenylphosphine)ruthenium(II),[22] and diisopropylphosphine[23] were prepared by literature methods. Tris(3-hydroxypropyl)phosphine was purchased from Strem and used without further purification. $LiAlH_4$ was purchased from Aldrich, and a concentrated solution in THF prepared by Soxhlet extraction. Air-sensitive NMR samples were prepared in an argon- or nitrogen-filled glovebox or on a high-vacuum line by vacuum transfer of solvent into an NMR tube fitted with a concentric Teflon valve. $^1$H, $^{13}C\{^1H\}$, and $^{31}P\{^1H\}$ spectra were recorded on Bruker DPX300, Avance III 400, Avance III 500, Avance III 600, or Avance III 700 NMR spectrometers operating at 300, 400, 500, 600, and 700 MHz for $^1$H, 100.61 or 150.92 MHz for $^{13}C\{^1H\}$, and 121.49, 161.98, 202.49, and 242.95 MHz for $^{31}P\{^1H\}$ respectively. All NMR spectra were recorded at 298 K, unless stated otherwise. $^1$H and $^{13}C\{^1H\}$ NMR spectra were referenced to residual solvent resonances. $^{31}P\{^1H\}$ NMR spectra were referenced to external neat trimethyl phosphite at 140.85 ppm. Dynamic NMR simulations were performed using WinDNMR: Dynamic NMR Spectra for Windows.[12] $T_1$ calculations were performed using the curve fitting applications of Origin 8.1, by OriginLab.[24] Microanalyses were carried out at the Campbell Microanalytical Laboratory, University of Otago, New Zealand. Details of the X-ray analyses are given in (Table 4).

**Synthesis of $P(CH_2CH_2CH_2P^iPr_2)_3$, $P^3P_3{}^{iPr}$ (1); $P(CH_2CH_2CH_2Br)_3$.** Phosphorus tribromide (4.5 mL, 0.048 mol) was added dropwise to a stirring suspension of tris(3-hydroxypropyl)phosphine (7.2 g, 0.035 mol) in DCM (30 mL) under nitrogen. The reaction mixture was stirred at room temperature for 18 h. Saturated aqueous sodium carbonate solution (approximately 30 mL) was added to the reaction mixture until all effervescence ceased. The organic layer was separated and dried over anhydrous sodium sulfate. The solution was filtered, and the solvent was removed under reduced pressure to give tris(3-bromopropyl)phosphine as a clear liquid (10.0 g, 73%). The crude $P(CH_2CH_2CH_2Br)_3$ was used immediately in the next step without further purification. $^{31}$P NMR (162 MHz, benzene-$d_6$): $\delta$ −34.1 (1P, sept, $^2J_{P-H}$ = 7 Hz). $^1H\{^{31}P\}$ NMR (400 MHz, benzene-$d_6$): $\delta$ 2.99 (6H, m, C**H**$_2$Br); 1.56 (6H, m, PC**H**$_2$); 1.06 (6H, m, CH$_2$C**H**$_2$CH$_2$). $^{13}C\{^1H\}$ NMR (101 MHz, benzene-$d_6$): $\delta$ 34.7 (d, $^3J_{C-P}$ = 14 Hz, **C**H$_2$Br); 29.4 (d, $^1J_{C-P}$ = 16 Hz, P**C**H$_2$); 25.5 (d, $^2J_{C-P}$ = 15 Hz, CH$_2$**C**H$_2$CH$_2$).

**LiP$^i$Pr$_2$.** Lithium phosphide was prepared following a modified method by Fryzuk et al.[25] *n*-Butyllithium (1.5 M in hexane, 50 mL, 0.097 mol) was added to diisopropylphosphine (8.3 g, 0.070 mol) in THF (40 mL) with stirring. This procedure resulted in a bright-yellow solution which was used directly in the next step.

**$P^3P_3{}^{iPr}$ (1).** The lithium diisopropylphosphide solution from the previous step was added to a stirring solution of tris(3-bromopropyl)-phosphine (10 g, 0.023 mol) in THF (approximately 100 mL). The reaction mixture was left to stir at room temperature for 18 h. The solvent was removed under reduced pressure, and benzene (20 mL) was added, followed by deaerated water (30 mL) which was added with care


dx.doi.org/10.1021/ic200492w |*Inorg. Chem.* 2011, 50, 6220–6228

at 0 °C until all excess lithium phosphide had been destroyed. Benzene (10 mL) was added, and the mixture was stirred for 2 h. The organic layer was decanted, dried over anhydrous sodium sulfate, and filtered to give a yellow solution. The solvent was removed under reduced pressure, and the resulting yellow oil was heated under vacuum (0.4 mbar) at 100 °C to remove volatile byproducts, leaving tris(3-diisopropylphosphinopropyl)phosphine as a yellow oil (9.0 g, 18 mmol, 51% from tris(3-hydroxypropyl)phosphine). $^{31}P\{^1H\}$ NMR (162 MHz, benzene-$d_6$): $\delta$ 1.9 (3P, s, $\mathbf{P}^i\mathrm{Pr}_2$); −34.7 (1P, s, $\mathbf{P}(CH_2)_3$). $^1H\{^{31}P\}$ NMR (400 MHz, benzene-$d_6$): $\delta$ 1.75 (6H, m, $CH_2\mathbf{CH_2}CH_2$); 1.58 (6H, m, $C\mathbf{H}(CH_3)_2$); 1.53 (6H, m, $PC\mathbf{H_2}$); 1.42 (6H, t, $^3J_{H-H}$ = 8 Hz, $PC\mathbf{H_2}$); 1.05 (18H, d, $^3J_{H-H}$ = 7 Hz, $CH(C\mathbf{H_3})_2$); 1.03 (18H, d, $^3J_{H-H}$ = 7 Hz, $CH(C\mathbf{H_3})_2$). $^{13}C\{^1H\}$ NMR (101 MHz, benzene-$d_6$): $\delta$ 29.8 (dd, $J_{C-P}$ = 12 Hz, 15 Hz, $P\mathbf{C}H_2$); 25.4 (dd, $J_{C-P}$ = 20 Hz, 14 Hz, $CH_2\mathbf{C}H_2CH_2$); 24.1 (dd, $J_{C-P}$ = 20 Hz, 10 Hz, $P\mathbf{C}H_2$); 23.7 (d, $^1J_{C-P}$ = 14 Hz, $\mathbf{C}H(CH_3)_2$); 20.4 (d, $^2J_{C-P}$ = 16 Hz, $CH(\mathbf{C}H_3)_2$); 19.0 (d, $^2J_{C-P}$ = 10 Hz, $CH(\mathbf{C}H_3)_2$). HRMS (EI) *m/z*: $[M + H]^+$ 509.3716 (calcd 509.3724)

**Synthesis of [RuCl($P^3P_3{}^{iPr}$)][$BPh_4$] (2[$BPh_4$]).** Tris(3-diisopropylphosphinopropyl)phosphine $P^3P_3{}^{iPr}$ (**1**) (456 mg, 0.896 mmol) was added to a brown solution of dichlorotris(triphenylphosphine)ruthenium-(II) (860 mg, 0.896 mmol) in THF (approximately 30 mL) resulting in an immediate color change to green. A stoichiometric amount of sodium tetraphenylborate (306 mg, 0.894 mmol) was added, and the solution slowly turned red with stirring. After 3 h, the solvent was removed under reduced pressure to give a pink solid which was recrystallized twice from THF layered with pentane (300 mg, 53%). Crystals suitable for X-ray diffraction were collected. Anal. found: C, 63.71; H, 8.27; $C_{51}H_{80}BClP_4Ru$ (MW 964.41) requires: C, 63.52; H, 8.36%. $^{31}P\{^1H\}$ NMR (162 MHz, THF-$d_8$): $\delta$ 25.7 (3P, br, $\mathbf{P_{E/T}}$); 14.2 (1P, q, $^2J_{P(C)-P(B/P)}$ = 36.4 Hz, $\mathbf{P_C}$). $^{31}P\{^1H\}$ NMR (243 MHz, 177.6 K, methylene chloride-$d_2$): $\delta$ 75.1 (Isomer-2, 1P, m, $\mathbf{P_B}$); 72.0 (Isomer-1, 1P, m, $\mathbf{P_B}$); 15.4 (Isomer-2, 1P, ddd, $^2J_{P(B)-P(D)}$ = 45 Hz, $^2J_{P(A)-P(D)}$ = 32 Hz, $^2J_{P(C)-P(D)}$ = 32 Hz, $\mathbf{P_D}$); 14.0 (Isomer-1, 1P, dt, m, $\mathbf{P_D}$); 4.1 (Isomer-1, 1P, dm, $^2J_{P(A)-P(C)}$ = 227 Hz, $\mathbf{P_A}$); 2.3 (Isomer-2, 1P, ddd, $^2J_{P(A)-P(C)}$ = 234 Hz, $^2J_{P(A)-P(D)}$ = 31 Hz, $^2J_{P(A)-P(B)}$ = 18 Hz, $\mathbf{P_A}$); −4.3 (Isomer-2, 1P, ddd, $^2J_{P(A)-P(C)}$ = 234 Hz, $^2J_{P(A)-P(D)}$ = 31 Hz, $^2J_{P(A)-P(B)}$ = 29 Hz, $\mathbf{P_C}$); −8.1 (Isomer-1, 1 P, dm, $^2J_{P(A)-P(C)}$ = 227 Hz, $\mathbf{P_C}$); $^1H$ NMR (400 MHz, THF-$d_8$): $\delta$ 7.29 (8H, m, $B\mathbf{Ph_{ortho}}$); 6.86 (8H, m, $B\mathbf{Ph_{meta}}$); 6.72 (4H, m, $B\mathbf{Ph_{para}}$); 2.64 (6H, sep, $^3J_{H-H}$ = 6.9 Hz, $C\mathbf{H}(CH_3)_2$); 1.96 (6H, m, $CH_2C\mathbf{H_2}CH_2$); 1.83 (6H, m, $P_{E/T}C\mathbf{H_2}$); 1.39 (9H, d, $CH(C\mathbf{H_3})$); 1.12 (9H, d, $CH(C\mathbf{H_3})$); 1.06 (6H, m, $P_CC\mathbf{H_2}$). $^{13}C\{^1H\}$ NMR (101 MHz, THF-$d_8$): $\delta$ 165.6 (m, $B\mathbf{Ph_{ipso}}$); 137.6 (s, $B\mathbf{Ph_{ortho}}$); 126.1 (m, $B\mathbf{Ph_{meta}}$); 122.2 (s, $B\mathbf{Ph_{para}}$); 30.8 (m, $\mathbf{C}H(CH_3)_2$); 29.1 (m, $P_{E/T}\mathbf{C}H_2$); 26.7 (m, $CH_2\mathbf{C}H_2CH_2$); 21.3 (s, $CH(\mathbf{C}H_3)$); 20.9 (s, $CH(\mathbf{C}H_3)$); 20.6 (m, $P_C\mathbf{C}H_2$).

**Synthesis of Ru($P^3P_3{}^{iPr}$)$H_2$ (3).** A suspension of potassium triethylborohydride (0.068 g, 0.49 mmol) and [RuCl($P^3P_3{}^{iPr}$)][$BPh_4$] (2[$BPh_4$]) (0.22 g, 0.23 mmol) was stirred in toluene (10 mL) overnight. The color of the pink suspension changed to a faint yellow. The suspension was filtered through Celite, and the solvent was removed under reduced pressure to give Ru($P^3P_3{}^{iPr}$)$H_2$ (**3**) as a white crystalline powder (0.101 g, 0.165 mmol, 72% yield). Crystals suitable for X-ray diffraction were grown by slow evaporation of a toluene solution under an atmosphere of nitrogen. Anal. found: C, 52.92; H, 10.51; $C_{27}H_{62}P_4Ru$ (MW 611.75) requires: C, 53.01; H, 10.22. $^{31}P\{^1H\}$ NMR (121.49 MHz, benzene-$d_6$): $\delta$ 49.2 (2P, dd, $^2J_{P(E)-P(C)}$ = 28.5 Hz, $^2J_{P(E)-P(T)}$ = 18.5 Hz, $\mathbf{P_E}$); 28.5 (1P, dt, $^2J_{P(T)-P(C)}$ = 28.5 Hz, $\mathbf{P_T}$); 0.4 (1P, dt, $\mathbf{P_C}$). $^1H$ NMR (400 MHz, toluene-$d_8$): $\delta$ 2.2−2.0 (2H, m, $C\mathbf{H}(CH_3)_2$); 2.0−1.9 (4H, m, $C\mathbf{H}(CH_3)_2$); 1.9−1.8 (6H, m, $C\mathbf{H_2}$); 1.8−1.7 (2H, m, $C\mathbf{H_2}$); 1.7−1.6 (4H, m, $C\mathbf{H_2}$); 1.5 (2H, m, $C\mathbf{H_2}$); 1.45−1.35 (4H, m, $C\mathbf{H_2}$); 1.3−1.15 (24H, m, $CH(C\mathbf{H_3})_2$); 1.15−1.05 (12H, m, $CH(C\mathbf{H_3})_2$); −9.43 (1H, dtdd, $^2J_{H-P}$ = 59.6 Hz, $^2J_{H-P}$ = 24.2 Hz, $^2J_{H-P}$ = 18.8 Hz $^2J_{H-H}$ = 6.2 Hz, Ru**H**); −12.50 (1H, dtdd, $^2J_{H-P}$ = 63.2 Hz, $^2J_{H-P}$ = 34.0 Hz, $^2J_{H-P}$ = 15.0 Hz, Ru**H**). $^{13}C\{^1H\}$ NMR (126 MHz, THF-$d_8$): $\delta$ 33.4 (s, $\mathbf{C}H(CH_3)_2$) ; 33.3 (s, $\mathbf{C}H(CH_3)_2$); 31.4 (dd, $J_{C-P}$ = 3.5 Hz, $J_{C-P}$ = 18 Hz, $P\mathbf{C}H_2$); 30.2 (t, $J_{C-P}$ = 16 Hz, $P\mathbf{C}H_2$); 30.0 (t, $J_{C-P}$ = 3.7 Hz, $CH_2\mathbf{C}H_2CH_2$); 29.8 (q, $J_{C-P}$ = 9 Hz, $P\mathbf{C}H_2$); 23.8 (t, $J_{C-P}$ = 4.7 Hz, $CH_2\mathbf{C}H_2CH_2$); 23.2 (d, $J_{C-P}$ = 5 Hz, $\mathbf{C}H(CH_3)_2$); 22.9 (dd, $J_{C-P}$ = 11 Hz, $J_{C-P}$ = 7 Hz, $P\mathbf{C}H_2$); 21.2 (s, $CH(\mathbf{C}H_3)_2$); 20.5 (s, $CH(\mathbf{C}H_3)_2$); 20.1 (s, $CH(\mathbf{C}H_3)_2$); 20.0 (s, $CH(\mathbf{C}H_3)_2$); 18.8 (s, $CH(\mathbf{C}H_3)_2$).

**Synthesis of [Ru($H_2$)(H)($P^3P_3{}^{iPr}$)][$BPh_4$] (4[$BPh_4$]).** A concentrated solution of $LiAlH_4$ in THF was added dropwise to a solution of [RuCl($P^3P_3{}^{iPr}$)][$BPh_4$] (2[$BPh_4$]) (0.16 g, 0.16 mmol) in THF (3 mL) until there was a color change from pink to colorless with a white suspension. Ethanol was added carefully, dropwise, until effervescence had ceased (about four drops) and the color of the reaction mixture had turned to orange, then an additional four drops of ethanol was added. The reaction mixture was filtered through Celite, and the solvent removed under reduced pressure. The orange powder was washed with pentane (10 mL) to give [Ru($H_2$)(H)($P^3P_3{}^{iPr}$)][$BPh_4$] (0.050 g, 0.051 mmol, 33% yield). Anal. found: C, 65.80; H, 8.98; $C_{51}H_{83}P_4RuB.C_4H_8O$ (MW 1004.10) requires: C, 65.79; H, 9.13. $^{31}P\{^1H\}$ NMR (203 MHz, THF-$d_8$): $\delta$ 24.7 (3P, s br, $\mathbf{P_{A/B/C}}$); 5.4 (1P, q, $^2J_{P-P}$ = 37.5 Hz, $\mathbf{P_D}$). $^{31}P\{^1H\}$ NMR (203 MHz, THF-$d_8$, 180K): $\delta$ 31.3 (1P, d br, $^2J_{P-P}$ = 185 Hz, $\mathbf{P_A}$); 21.3 (1P, d br, $^2J_{P-P}$ = 185 Hz, $\mathbf{P_A}$); 13.7 (1P, s br, $\mathbf{P_C}$); 4.3 (1P, s br, $\mathbf{P_D}$). $^1H$ NMR (400 MHz, THF-$d_8$): $\delta$ 7.20 (8H, m, $B\mathbf{Ph_{ortho}}$); 6.82 (8H, m, $B\mathbf{Ph_{meta}}$); 6.68 (4H, m, $B\mathbf{Ph_{para}}$); 2.1−1.9 (12H, m, $C\mathbf{H}(CH_3)_2/C\mathbf{H_2}$); 1.9−1.8 (6H, m, $C\mathbf{H_2}$); 1.65−1.55 (6H, m, $C\mathbf{H_2}$); 1.25−1.05 (36H, m, $CH(C\mathbf{H_3})_2$); −8.57 (3H, s br, Ru($\mathbf{H_2}$)(**H**)). $^1H$ NMR (600 MHz, THF-$d_8$, 195 K, high field only): $\delta$ −7.44 (2H, s br, Ru($\mathbf{H_2}$)); $\delta$ −10.29 (1H, dt br, $^2J_{H-P}$ = 57 Hz, $^2J_{H-P}$ = 32 Hz, Ru(**H**)). $^{13}C\{1H\}$ NMR (151 MHz, THF-$d_8$): $\delta$ 165.1 (m, $B\mathbf{Ph_{ipso}}$) 137.0 (s, $B\mathbf{Ph_{meta}}$); 125.4 (m, $B\mathbf{Ph_{ortho}}$); 121.6 (s, $B\mathbf{Ph_{para}}$); 30.2 (s br, $\mathbf{C}H(CH_3)_2$); 29.0 (d, $^1J_{C-P}$ = 32 Hz, $P_{E/T}\mathbf{C}H_2$); 25.9 (m, $P_C\mathbf{C}H_2$); 21.1 (s, $CH_2\mathbf{C}H_2CH_2$); 19.8 (s, $CH(\mathbf{C}H_3)_2$); 19.2 (s, $CH(\mathbf{C}H_3)_2$).

## ■ ASSOCIATED CONTENT

**Supporting Information.** A CIF file with crystallographic data for compounds [RuCl($P^3P_3{}^{iPr}$)][$BPh_4$]·THF (2[$BPh_4$]), [$RuH_2$($P^3P_3{}^{iPr}$)] (**3**), and Ru($H_2$)(H)($P^3P_3{}^{iPr}$)][$BPh_4$]·EtOH (4[$BPh_4$]). This material is available free of charge via the Internet at http://pubs.acs.org.

## ■ AUTHOR INFORMATION

**Corresponding Author**

*E-mail: L.Field@unsw.edu.au. Telephone: +61 2 9385 2700.

## ■ ACKNOWLEDGMENT

The authors wish to thank Dr. Hsiu Lin Li and Dr. Alison Magill for technical assistance and discussions. The authors also thank the Australian Research Council for financial support, and R.G.-W. thanks the Australian Government and the University of New South Wales for postgraduate scholarships.

## ■ REFERENCES

(1) Mayer, H. A.; Kaska, W. C. *Chem. Rev.* **1994**, *94*, 1239–72.

(2) (a) Field, L. D.; Guest, R. W.; Vuong, K. Q.; Dalgarno, S. J.; Jensen, P. *Inorg. Chem.* **2009**, *48*, 2246–2253. (b) Bianchini, C.; Perez, P. J.; Peruzzini, M.; Zanobini, F.; Vacca, A. *Inorg. Chem.* **1991**, *30*, 279–287.

(3) Masters, C., *Homogeneous Transition-metal Catalysis*; University Press: Cambridge, U.K., 1981.

(4) Sung, K.-M.; Huh, S.; Jun, M.-J. *Polyhedron* **1998**, *18*, 469–479.

(5) Pascariu, A.; Iliescu, S.; Popa, A.; Ilia, G. *J. Organomet. Chem.* **2009**, *694*, 3982–4000.
(6) (a) Bampos, N.; Field, L. D. *Inorg. Chem.* **1990**, *29*, 587–8. (b) Bampos, N.; Field, L. D.; Messerle, B. A. *Organometallics* **1993**, *12*, 2529–35. (c) Field, L. D.; Bampos, N.; Messerle, B. A. *Magn. Reson. Chem.* **1991**, *29*, 36–9. (d) Antberg, M.; Frosin, K. M.; Dahlenburg, L. *J. Organomet. Chem.* **1988**, *338*, 319–27. (e) Antberg, M.; Prengel, C.; Dahlenburg, L. *Inorg. Chem.* **1984**, *23*, 4170–4.
(7) (a) Bianchini, C.; Bohanna, C.; Esteruelas, M. A.; Frediani, P.; Meli, A.; Oro, L. A.; Peruzzini, M. *Organometallics* **1992**, *11*, 3837–3844. (b) Bianchini, C.; Meli, A.; Peruzzini, M.; Frediani, P.; Bohanna, C.; Esteruelas, M. A.; Oro, L. A. *Organometallics* **1992**, *11*, 138–45. (c) Field, L. D.; Messerle, B. A.; Smernik, R. J. *Inorg. Chem.* **1997**, *36*, 5984–5990. (d) Field, L. D.; Messerle, B. A.; Smernik, R. J.; Hambley, T. W.; Turner, P. *Inorg. Chem.* **1997**, *36*, 2884–2892.
(8) Addison, A. W.; Rao, T. N.; Reedijk, J.; Vanrijn, J.; Verschoor, G. C. *J. Chem. Soc., Dalton Trans.* **1984**, 1349–1356.
(9) Brookhart, M.; Green, M. L. H.; Parkin, G. *Proc. Natl. Acad. Sci. U.S.A.* **2007**, *104*, 6908–6914.
(10) (a) Antberg, M.; Dahlenburg, L. *Inorg. Chim. Acta* **1986**, *111*, 73–6. (b) Antberg, M.; Dahlenburg, L. *Acta Crystallogr., Sect. C: Cryst. Struct. Commun.* **1986**, *C42*, 997–9. (c) Dahlenburg, L.; Frosin, K. M. *Polyhedron* **1993**, *12*, 427–34.
(11) (a) Garrou, P. E. *Inorg. Chem.* **1975**, *14*, 1435–1439. (b) Garrou, P. E. *Chem. Rev.* **1981**, *81*, 229–66.
(12) Reich, H. J. *WinDNMR: Dynamic NMR Spectra for Windows*; University of Wisconsin: Madison, WI, 1998.
(13) (a) Nicasio, M. C.; Perutz, R. N.; Walton, P. H. *Organometallics* **1997**, *16*, 1410–1417. (b) Mebi, C. A.; Frost, B. J. *Inorg. Chem.* **2007**, *46*, 7115–7120.
(14) Lough, A. J.; Morris, R. H.; Ricciuto, L.; Schleis, T. *Inorg. Chim. Acta* **1998**, *270*, 238–246.
(15) Bianchini, C.; Masi, D.; Peruzzini, M.; Casarin, M.; Maccato, C.; Rizzi, G. A. *Inorg. Chem.* **1997**, *36*, 1061–1069.
(16) Matthes, J.; Grundemann, S.; Toner, A.; Guari, Y.; Donnadieu, B.; Spandl, J.; Sabo-Etienne, S.; Clot, E.; Limbach, H.-H.; Chaudret, B. *Organometallics* **2004**, *23*, 1424–1433.
(17) Toner, A. J.; Gründemann, S.; Clot, E.; Limbach, H.-H.; Donnadieu, B.; Sabo-Etienne, S.; Chaudret, B. *J. Am. Chem. Soc.* **2000**, *122*, 6777–6778.
(18) Morris, R. H. *Coord. Chem. Rev.* **2008**, *252*, 2381–2394.
(19) Gusev, D. G. *J. Am. Chem. Soc.* **2004**, *126*, 14249–14257.
(20) (a) Baker, M. V.; Field, L. D.; Young, D. J. *J. Chem. Soc., Chem. Commun.* **1988**, 546–8. (b) Chinn, M. S.; Heinekey, D. M. *J. Am. Chem. Soc.* **1987**, *109*, 5865–5867. (c) Cappellani, E. P.; Drouin, S. D.; Jia, G. C.; Maltby, P. A.; Morris, R. H.; Schweitzer, C. T. *J. Am. Chem. Soc.* **1994**, *116*, 3375–3388.
(21) Perrin, D. D. A., W., L. F. *Purification of Laboratory Chemicals*; 3rd ed.; Pergamon Press: Oxford, U.K., 1993.
(22) Hallman, P. S.; Stephenson, T. A.; Wilkinson, G. *Inorg. Synth.* **1970**, *12*, 237–40.
(23) Zhu, K.; Achord, P. D.; Zhang, X.; Krogh-Jespersen, K.; Goldman, A. S. *J. Am. Chem. Soc.* **2004**, *126*, 13044–13053.
(24) *Origin 8.1 SR2*; Originlab Corporation: Northhampton, MA, 2010.
(25) Fryzuk, M. D.; Carter, A.; Westerhaus, A. *Inorg. Chem.* **1985**, *24*, 642–8.